# STRUCTURAL STATES OF MYELIN OBSERVED BY X-RAY DIFFRACTION AND FREEZE-FRACTURE ELECTRON MICROSCOPY

D. A. KIRSCHNER, C. J. HOLLINGSHEAD, C. THAXTON, D. L. D. CASPAR, and D. A. GOODENOUGH

From the Structural Biology Laboratory, Rosenstiel Basic Medical Sciences Research Center, Brandeis University, Waltham, Massachusetts 02154, and the Department of Anatomy, Harvard Medical School, Boston, Massachusetts 02115. Dr. Kirschner's present address is the Department of Neuroscience, Children's Hospital Medical Center, Boston, Massachusetts 02115.

ABSTRACT

Coordinated freeze-fracture electron microscopy and x-ray diffraction were used to visualize the morphological relation between compacted and native period membrane arrays in myelinated nerves treated with dimethylsulfoxide (DMSO). Comparison of x-ray diffraction at room temperature and at low temperature was used as a critical measure of the extent of structural preservation. Our x-ray diffraction patterns show that in the presence of cryoprotective agents, it is possible to preserve with only small changes the myelin structure which exists at room temperature. These changes include a slight increase in packing disorder of the membranes, a small, negative thermal expansion of the membrane unit, and some reorganization in the cytoplasmic half of the bilayer. The freeze-fracture electron microscopy clearly demonstrates continuity of compact and native period phases in DMSO-treated myelin. Finally, the use of freezing to trap the transient, intermediate structure during a structural transition in glycerol is demonstrated.

KEY WORDS x-ray diffraction · freeze-fracture electron microscopy · cryoprotection · frozen myelin · structural preservation · compacted myelin structure

Our freeze-fracture studies on myelin structure were begun to see how the sheath is reorganized in the process of membrane compaction after treatment with dimethylsulfoxide (DMSO) (12). X-ray patterns from nerves bathed for ~½ h in Ringer's solution containing 10% or more DMSO (vol/vol) show reflections from a new, highly ordered membrane array with a repeat period of ~120 Å. This distinct phase coexists with membrane arrays having the 180-Å native period in mammalian peripheral nerve. The proportion of compacted membranes is greater at higher DMSO concentrations, and above 40% DMSO, the native phase is no longer observed. Replacing the DMSO with Ringer's solution leads to the rapid reappearance of the native diffraction pattern. DMSO appears to draw the membrane bilayers closer together by lowering the water activity. X-ray diffraction patterns show that similar close-packed arrays are formed when myelin is dehydrated by evaporation or by contact with a variety of hypertonic solutions.

Two fundamental questions are addressed in



J. CELL BIOLOGY © The Rockefeller University Press · 0021-9525/79/07/0140/10 $1.00
Volume 82 July 1979 140–149

the current study. First, at the tissue level, what is the relation of compacted and native period domains and how is the compacted structure formed from the native? Since conventional fixation and embedding for electron microscopy introduce artifacts such as general shrinkage and lipid extraction (reviewed in reference 22), we chose freeze-fracture as a method that might preserve the morphology for direct observation of distinct membrane arrays in the electron microscope. Second, at the molecular level, how well does freezing preserve structure? Some artifacts may be introduced by freezing, but there has been little direct comparison of what one sees with freeze-fracture with what one sees by x-ray diffraction. Structural perturbations from freezing have been previously examined in model lipid-water and lipid-protein-water systems using x-ray diffraction (6).

In approaching these questions, we have compared freeze-fracture and x-ray diffraction from myelin treated with different concentrations of DMSO; and have examined conventionally cryoprotected nerve after different times in glycerol.

## MATERIALS AND METHODS

### *Specimens*

Sciatic nerves, dissected from normal mature mice, were mounted under tension on stainless-steel yokes and stored up to 5 h at room temperature in solutions that included normal saline, 3, 10, or 20% DMSO-saline, or 20% glycerol-saline. Some of the nerves were frozen in a liquid nitrogen-cooled Freon 22 slush and stored in liquid nitrogen.

### *X-Ray Diffraction*

The frozen nerve, mounted on a yoke, was positioned in a stream of cold, dry nitrogen gas provided by the controlled boiling of liquid nitrogen in two steel-sheathed ceramic heaters arranged in the shape of a U-tube and connected directly to the outlet of a liquid nitrogen tank kept at a head pressure of 18 lb/in$^2$. The cold gas stream was maintained below −160° as indicated by the presence of frozen Freon 22 on the specimen. Condensation of ambient moisture was minimized by surrounding the nitrogen stream with a coaxial stream of dry air.

Diffraction patterns, obtained on a double-mirror camera using the $CuK_\alpha$ radiation from an Elliott rotating anode generator (Marconi-Elliott Avionic Systems, Ltd., Borehamwood, Herts, England) operated at 40 kV × 18 mA, were recorded on Ilford Industrial G film (Ilford Ltd., Ilford, Essex, England). The specimen-to-film distance was 13–14 cm. Exposure times of ~30 min were sufficient for recording the strong small-angle scatter; longer exposures were used to record the weak, higher angle diffraction. The optical densities of the diffraction patterns were measured on a 25-μm raster with a rotating drum scanner, the Optronics Photoscan P-1000 (Optronics International, Inc., Chelmsford, Mass.). The measurements were then averaged over 10–20° arcs at constant radius from the center of the diffraction patterns. Background was estimated for each peak from a fourth order polynomial fit to the intensity minima on either side of the reflections. Integrated intensities of the reflections $I(h)$, where $h$ is the order number, were measured by numerical integration of the area under the peaks after background substraction. Structure amplitudes $F(h)$ were calculated from $\sqrt{h^2 I(h)}$ where $h^2$ is the Lorentz factor derived for the point-focus geometry of the experiment (20). The relative structure factors for the different diffraction patterns were scaled by setting $\sum_h F^2(h)/d =$ constant. This is equivalent to equating the integrals of the squares of the electron density fluctuations. Phases were assigned to the structure factors for the DMSO-compacted myelin as previously determined (11).

A refinement procedure was used to calculate and compare the electron density profiles from compacted myelin at room temperature and frozen (Fig. 10). Unobserved reflections do not generally have zero intensity; rather, they are below the level of detectability. Details of the profile do, however, depend on including them in the Fourier synthesis. For example, the seventh order is above the level of detectability in the room temperature pattern, but below in the pattern from frozen myelin. If the seventh-order structure factor is set equal to zero in calculating the membrane profile, the two membrane profiles are significantly different. However, if this structure factor is given a finite value that is still below the level of detectability, then the differences in the membrane profiles are reduced. Accordingly, the structure factors for the two patterns were varied within their measured uncertainties to minimize the differences between the two profiles.

### *Electron Microscopy*

The unfrozen nerves, previously examined at room temperature by x-ray diffraction, were cut into segments 1–2 mm long and placed on 3-mm-diameter paper disks. The specimens were then frozen in a liquid nitrogen-cooled Freon 22 slush and freeze-fractured in a Balzers BAF 301 freeze-fracture apparatus (Balzers Corp., Nashua, N. H.) according to standard techniques. After overnight storage in methanol, the replicas were cleaned in $Clorox_R$, mounted on uncoated copper grids, and examined in a Philips 301 electron microscope. For comparing repeat periods, optical diffraction patterns were obtained from selected areas of the micrographs from the replicas. Negatively stained tropomyosin paracrystals, having a repeat period of 395 ± 5 Å as determined by x-ray diffraction, were used to calibrate the magnification of the micrographs.

## RESULTS

### *Diffraction from DMSO-Treated and Untreated Myelin*

The characteristic myelin equatorial reflections observed at room temperature (Fig. 1*a*) disappear when an uncryoprotected nerve is frozen at liquid nitrogen temperature. The strong diffuse scatter extending from ~62- to 74-Å spacing and the weak scatter at ~48 Å which are observed (Fig. 1 *b*) indicate that the lamellar structure is disrupted when the sample is frozen. This strong diffuse scatter presumably arises from variable packing of membrane bilayers induced by ice formation in the myelin lattice.

Diffraction patterns from nerves bathed in saline solution containing DMSO at concentrations of 10% or more show the coexistence of compacted and native membrane arrays over a temperature range of ~5°–55°C (12). In the current study, the diffraction pattern from a nerve treated with 20% DMSO-saline and examined at room temperature (Fig. 1 *c*) shows a repeat period of 121 Å with Bragg orders 1, 2, 3, 4, 7, 8 observed for the compacted phase, and 174 Å with orders 1, 2, 4, 5 for the native phase. The diffraction pattern from this nerve when subsequently frozen and examined at liquid nitrogen temperature (Fig. 1 *d*) continues to show the two sets of lamellar reflections but with repeat periods slightly larger than at room temperature: the 126-Å period compacted phase with Bragg orders 2, 3, 4, 8 and the 188-Å period native phase with orders 2, 4, 5. The difference in repeat periods between the compacted membrane arrays at room temperature and when frozen correlates with changes in the diffracted

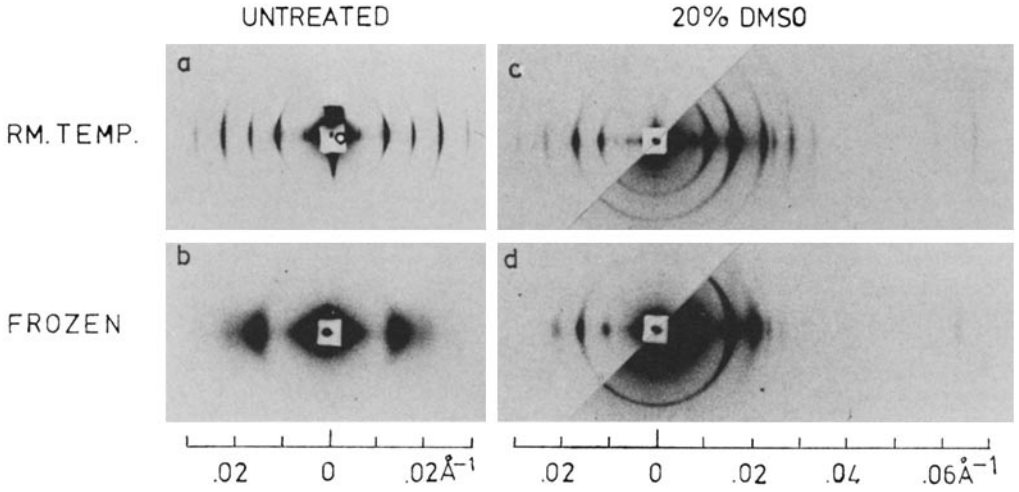


FIGURE 1 X-ray diffraction patterns of myelin from DMSO-treated and untreated mouse sciatic nerves at room temperature and frozen at liquid nitrogen temperature. (*a*) Nerve in normal saline at room temperature shows a myelin periodicity of 177 Å with orders 1–5 detectable (1.3-h x-ray exposure). (*b*) Nerve frozen in normal saline shows no myelin periodicity (1.5-h x-ray exposure). The small-angle scatter around the central beam stop is intensified, and a broad intensity maximum extends from ~0.01 to 0.025 $Å^{-1}$. (*c*) Nerve at equilibrium in 20% DMSO-saline solution at room temperature (6.9-h x-ray exposure) shows a 121-Å period compacted phase with orders 1, 2, 3, 4, 7, 8 and 174-Å period native phase with orders 1, 2, 4, 5. The relative diffracting powers of the two sets of reflections indicates that ~60% of the ordered myelin is in the compacted phase. (*d*) DMSO-treated nerve frozen and examined at liquid nitrogen temperature (2-h x-ray exposure) continues to show discrete orders 2, 3, 4, 8 from a 126-Å period compacted phase, and orders 2, 4, 5 from a 188-Å period native phase. The first-order reflections are obscured by the intense, low-angle diffuse scatter. The relative diffracting powers indicate that ~70% of the myelin is in the compacted phase. For the DMSO-treated specimens (*c* and *d*), top films as well as underfilms have been included to show the discrete reflections of the compacted and native phases, particularly between 0.06 and 0.07 $Å^{-1}$ (15- to 16-Å spacing). The diffracting power of frozen myelin appeared to be consistently greater than that of myelin at room temperature, both for untreated specimens as well as for DMSO-treated nerves. Quantitative measurements using a counter are required to explore this phenomenon.

intensity distribution. The increase in line-width of the diffraction orders from frozen myelin compared to those from similarly treated myelin at room temperature indicates that the periodicity of the membrane arrays is somewhat more variable when frozen, but the discrete reflections at ~15-Å spacing show that the regularity is retained to at least this resolution in the frozen tissue.

At DMSO concentrations <20%, the structure is not well preserved when frozen. At 3% DMSO-saline, very strong diffuse scatter is centered at ~72-Å spacing, with weaker intensity maxima visible at 64-, 52-, and 39-Å spacings. At 10% DMSO the first four orders of a lattice with repeat period ~181 Å are detected as discrete reflections, as well as a weak, diffuse reflection at ~73-Å spacing which would correspond to the second order of a slightly compacted lattice. The strong, diffuse background scatter from these frozen specimens at lower DMSO concentrations indicates that most of the myelin sheath is comprised of disrupted membrane arrays.

### *Freeze-Fracture Observations on DMSO-Treated and Untreated Myelin*

Replicas of cross-fractured, noncryoprotected myelin show that most of the membrane arrays in the sheath are disrupted by freezing, although a few ordered regions remain (Fig. 2). *En face* views show considerable rippling in the plane of the membrane that is presumably caused by ice crystal formation in the spaces between membrane layers. In contrast, replicas of myelin that have been frozen after treatment with 20% DMSO-saline solution (Fig. 4) show preservation of well-ordered membrane arrays having repeat periods corresponding to those measured from the X-ray diffraction patterns. Optical diffraction patterns of the electron micrographs (Fig. 4, insets) show the first four orders for both the native and the compacted membrane arrays. The presence of odd orders shows that the pairing of the membranes is retained in the compacted array.

The fraction of the membrane surface in smooth, close-packed layers (Fig. 3) increases with increasing concentration of DMSO. Correspondingly, x-ray diffraction patterns (12) show that as the DMSO concentration increases, an increasing proportion of compacted myelin co-exists with a decreasing proportion of normal period arrays. The electron micrographs clearly demonstrate continuity of the membranes between these two types of layering in the sheath. A freeze-fracture study of myelin in which compacted arrays have been formed by a variety of treatments indicates that the intramembrane particles are always laterally displaced from the compacted membrane domains and concentrated in the normal period arrays (1).

### *Diffraction from Gycerol-Treated Myelin*

Sciatic nerve was treated for ~2.5 h at room temperature with 20% glycerol-saline solution and then frozen and examined at liquid nitrogen temperature. The x-ray pattern (Fig. 5 *b*) shows the coexistence of two lamellar phases. Discrete, somewhat broadened second and fourth orders from a compacted 130-Å phase, as well as the first, second, and fourth orders from a 190-Å phase are observed. Sciatic nerve frozen after 5-h treatment, however, shows only a single phase indicated by the first five orders of a 186-Å repeat. The possibility that sciatic myelin undergoes a transient compaction as it is glycerinated was examined at room temperature by recording serial x-ray patterns from nerves perfused with 20% glycerol-saline. Within 30 min (Fig. 5 *a*) a reflection at 65-Å spacing appears. This new reflection is clearly distinguished from the third-order reflection from the native lattice that is observed at a spacing of 59 Å before treatment and at 58.3 Å after treatment in glycerol solution. After ~1 h the new reflection increases in intensity and shifts in position to ~63-Å spacing. With continued perfusion for between 2 and 3 h, however, this reflection is no longer detected, and only reflections from the 176-Å period native lattice are observed. The transient reflection observed at room temperature at spacings 63–65 Å is the second order of the compacted membrane array. Therefore, glycerol induces a transient structural heterogeneity in myelin at room temperature, and freezing can be used to trap these structural states before equilibrium is attained (Fig. 5 *b*).

### *Freeze-Fracture of Glycerol-Treated Nerves*

Observations on freeze-fracture replicas of myelin that has been frozen after treatment with 20% glycerol-saline parallel the results of x-ray diffraction. After 15-min treatment, well-defined compacted and native membrane arrays are seen in cross-fracture (Fig. 6). Views of internal membrane faces show a corresponding delineation of

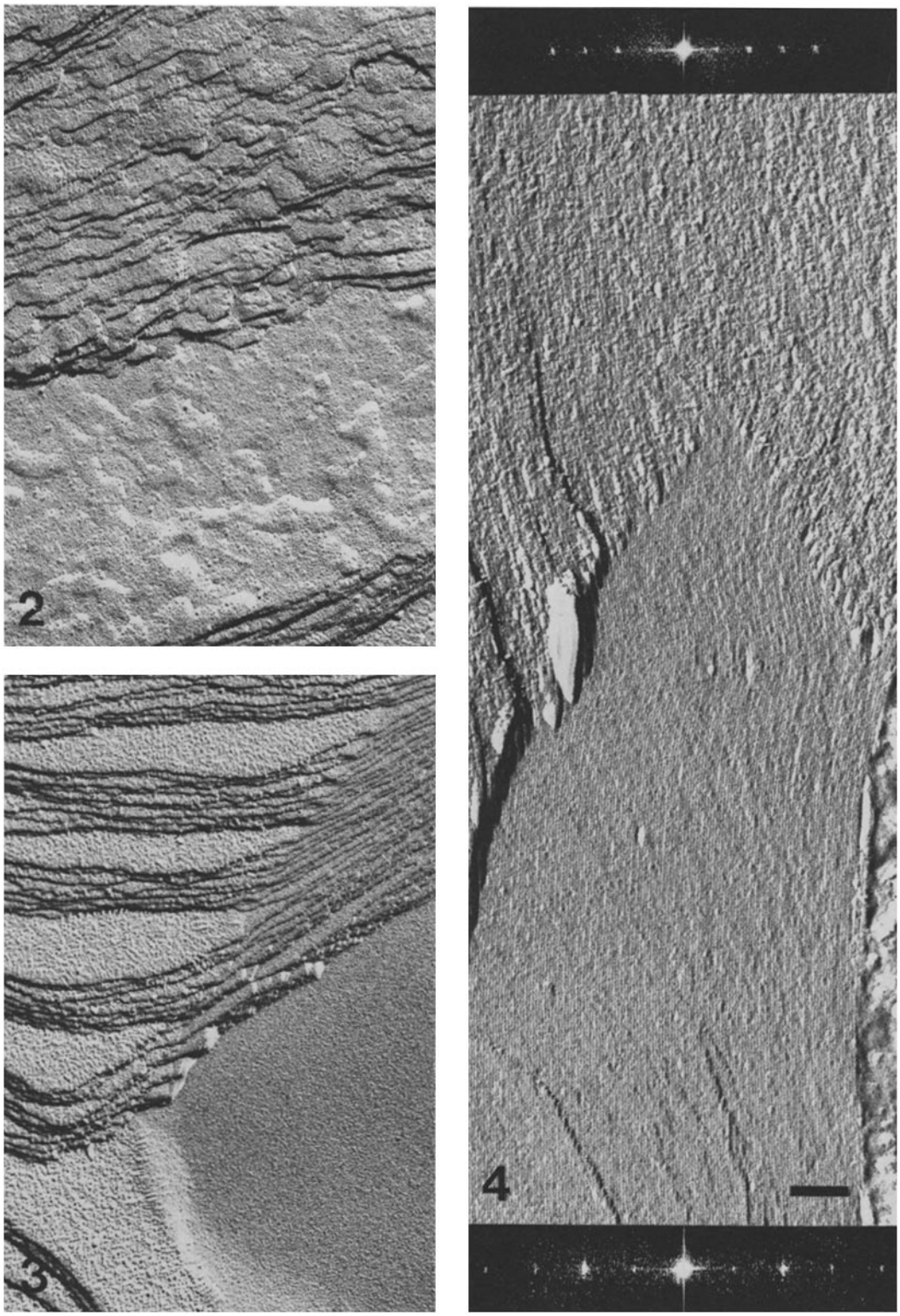
2
3
4

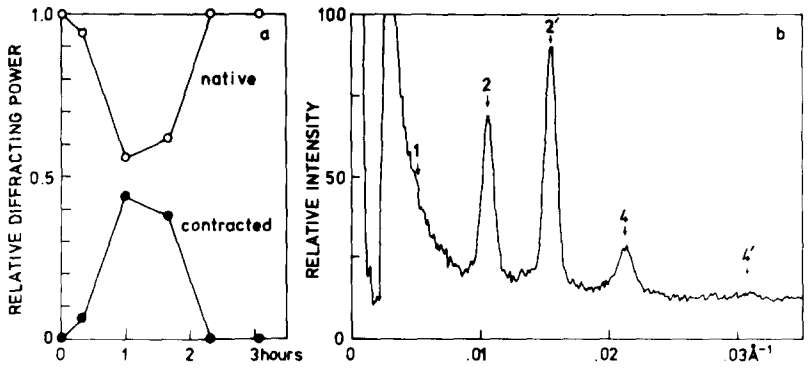


FIGURE 5 (*a*) X-ray diffraction measurements at room temperature from sciatic nerve perfused with 20% glycerol-saline solution. The relative proportion of membrane in the native and compacted phases is expressed by the relative diffracting power as a function of time from the start of perfusion. After ~2- to 3-h treatment, the compacted phase is no longer detected. (*b*) Densitometer tracing of a diffraction pattern from sciatic nerve frozen at liquid nitrogen temperature after 2.5 h in 20% glycerol-saline at room temperature. The slightly different kinetics between this specimen and that used in Fig. 5 *a* might be a consequence of specimen variability as well as differences in perfusion conditions. The pattern shows a 190-Å period phase with orders 1, 2, 4 and a 130-Å compacted phase with orders 2', 4'.

particle-free and particle-rich domains (Fig. 7). After ~2–3 h in the glycerol solution, however, only a single well-defined array having a native period is observed in cross-fracture (Fig. 8), and homogenous, particulate membrane faces are seen in *en face* views (Fig. 9). Our results explain the observations of Branton (2) that sciatic nerve myelin in 20% glycerol-saline shows large domains of smooth fracture faces. The nerves in that study were reportedly frozen within 20 min after glycerol treatment, and, therefore, according to our findings, would show significant formation of compacted, particle-free membrane arrays.

### *Membrane Structure at Low and Ambient Temperature*

Electron density profiles of the membranes in myelin compacted at room temperature and subsequently frozen were calculated (Fig. 10) using diffraction data to ~15-Å spacing with phases previously determined for the DMSO-compacted array (11). The peroid for the membrane pair increases from 121 to 126 Å on freezing. This difference can be accounted for by a uniform expansion of the membrane units by ~4 Å plus an increase of ~1 Å in the separation of the cytoplas-

---

FIGURES 2–4 Freeze-fracture electron microscopy on DMSO-treated and untreated sciatic nerve. Bar, 0.1 μm. × 90,500.

FIGURE 2 An oblique view of fresh frozen, untreated myelin. The fracture faces are rippled due to disruption by the formation of ice crystals, but the small particles are evenly dispersed across the face.

FIGURE 3 An oblique view from myelin treated with 20% DMSO for 2 h. A transition zone between a smooth, particle-free membrane array (right) and a particle-rich array (left) is shown. These correspond respectively to the compacted and native period domains seen in cross-fracture.

FIGURE 4 A cross-fracture from the same replica as Fig. 3. The smooth fracturing, compacted array (bottom) has a period of ~120 Å and is continuous with the rough membrane array (top) which has a native period of ~180 Å. The optical diffraction patterns at top and bottom were taken from the areas to which they are adjacent and show very clearly the difference in period. The pairing of membranes in the compacted and normal period arrays can be seen by viewing the micrograph edge on from the bottom and top, respectively.

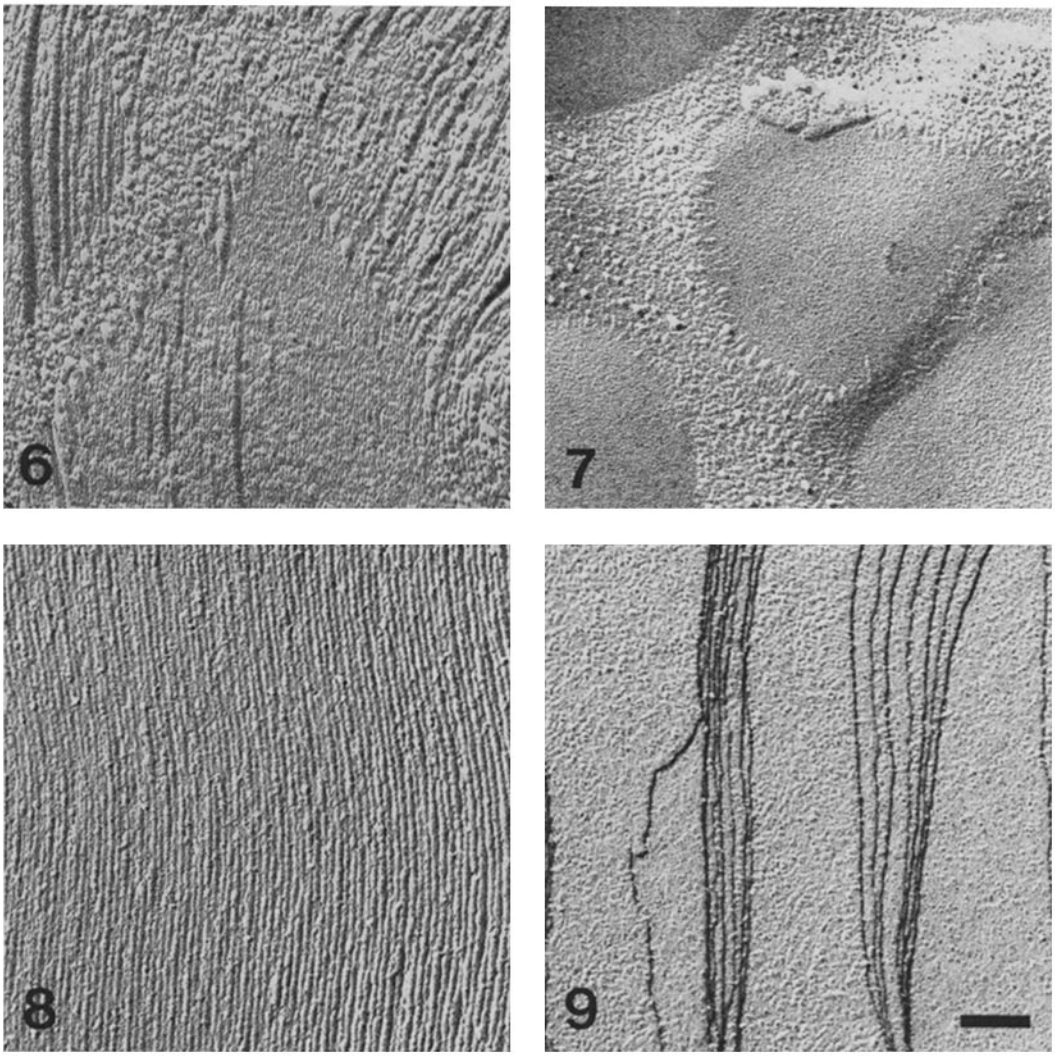


FIGURES 6–9 Freeze-fracture electron microscopy on glycerol-treated sciatic nerves. Bar, 0.1 μm. × 90,500.

FIGURE 6 A cross-fracture from a replica of myelin treated with 20% glycerol for 15 min. Smooth, compacted array (bottom and upper left) is continuous with rough, native-period array (top).

FIGURE 7 An *en face* view of the membrane from the same replica as Fig. 6. A network of particle-rich membrane surrounds smooth, particle-free areas.

FIGURE 8 A cross-fracture from a replica of myelin treated with 20% glycerol for 3 h. A single membrane array having a native period is seen.

FIGURE 9 An oblique view from a replica of myelin treated with 20% glycerol for 2 h. Particles are evenly dispersed over the membrane faces.

mic membrane surfaces. Calculating the profile of the low temperature form with a 3% shrinkage and comparing this with that at room temperature show that the external halves of the bilayers at the two temperatures can be superimposed after adjusting for the thermal expansion. There are, however, localized differences in the region of the high density polar layer and the steroid step in the

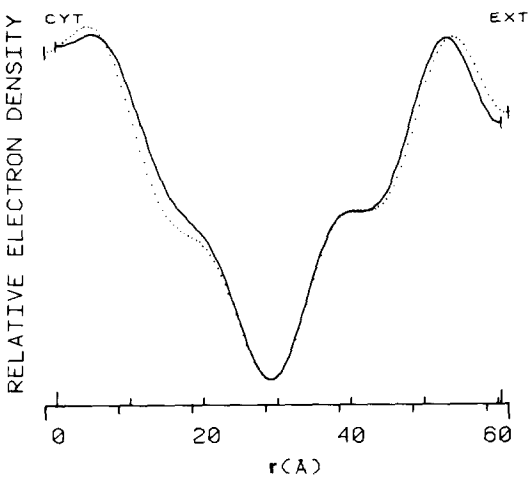


FIGURE 10 Electron density profiles of the membranes in DMSO-compacted myelin at room temperature (solid curve) and frozen (dotted curve). The profiles were calculated from the diffraction data to ~15-Å spacing (Fig. 1 *c* and *d*). The membrane unit at room temperature is 60.5 Å wide, and 63 Å when frozen. The upper scale marks refer to the room temperature profile, and the lower to the profile at low temperature. The origins of the two profiles have been shifted to align the centers of the membrane profiles. The origin on the left is the cytoplasmic boundary between membrane bilayers; and the external boundary is on the right. Since the first-order reflection is obscured by small-angle diffuse scatter in the frozen specimen, the first-order harmonics were not included in the calculated profiles.

cytoplasmic half of the bilayer between the profiles at low and high temperatures. On lowering the temperature, the density in the steroid step region decreases and the step becomes flatter; the density decrease in this region is compensated for by an increase in the polar peak.

## DISCUSSION

### *Relation between Compact and Normal Period Domains*

Replicas of cross-fractured myelin that have been treated with 20% DMSO-saline to induce compaction of membrane arrays clearly show that the membrane layering is continuous between the compact and normal period domains (Fig. 4). Compaction in myelin that is induced by DMSO and similar dehydrating treatments must proceed, therefore, by a local recrystallization of the membrane arrays rather than by winding up the spiral wrapping (12). Freeze-fracture electron microscopy shows that myelin compaction always leads to a segregation of particles from the compacted domains (1). Intramembrane particles, visualized by freeze-fracture, correlate with the presence of defined proteins in reconstituted pure lipid bilayers, and the particle density parallels the protein content of biological membranes (reviewed in reference 22). The particle-free compact and particle-enriched normal period domains in myelin, therefore, have distinct chemical compositions.

### *Structural Preservation by Freezing*

The conventional technique of freezing tissue by immersion in a Freon 22 slush at liquid nitrogen temperature produces disruption of both short- and long-range order in myelin due to microcrystalline ice formation (Fig. 1 *b* and 2). With cryoprotection, however, freezing in this way induces very little structural change in myelin as shown by x-ray patterns at room temperature and frozen (Fig. 1 *c* and *d*; Fig. 5).An x-ray pattern from a nerve ~0.5–1 mm in diameter averages the diffraction from $\sim 10^2$–$10^3$ myelin sheaths. The patterns indicate that molecular organization is preserved throughout the cryoprotected, frozen tissue. The use of cryoprotectants may, however, produce artifacts. For example, DMSO induces membrane compaction (12) and particle segregation (1) in myelin, while glycerol leads to a transient structural transition (Figs. 5–7). Such effects may be avoided by using ultrafast freezing with liquid helium which has been shown to preserve the superficial layers in a tissue block (10).

### *Molecular Organization in Compacted Myelin*

Freeze-fracture electron microscopy shows that myelin membranes have numerous intramembrane particles (17), whereas experimentally compacted myelin membranes are particle-free (1). These particles probably represent transmembrane proteins. In myelin, such protein could provide polar protrusions for bridging between the membrane lamellae and act like struts to support the normal period. When this protein is displaced, the membrane layers would come closer together, resulting in compacted myelin. The smooth fracture faces of compacted myelin (Figs. 3 and 7) indicate that there is little or no intramembrane protein in the compacted arrays.

The transmembrane protein is likely to be the glycoprotein which is amphiphilic (3, 4, 14), and

which comprises ~50% of the total protein in peripheral nervous system (PNS) myelin (7, 9, 21). In all, protein represents ~18% of the anhydrous weight of PNS myelin (9), or 16% by volume (13). Since the water content of PNS myelin is 40–45% by volume (5, 12), then protein occupies ~9% and the glycoprotein ~4.5% of the hydrated volume of peripheral myelin. The average volume fraction of protein in the hydrocarbon layer is estimated from neutron diffraction measurements to be 4–9% (13). Therefore, there is sufficient glycoprotein to account for the protein traversing the lipid hydrocarbon of the membrane bilayer in PNS myelin.

The electron density profile of DMSO-compacted myelin (Fig. 10) shows an asymmetric membrane unit with thickness similar to that of the symmetric bilayer formed by purified myelin lipids (V. Melchior, C. J. Hollingshead, and D. L. D. Caspar, manuscript in preparation). The shape of the centrosymmetrically averaged compacted myelin profile resembles that of lecithin-cholesterol (8, 16, 18) and myelin lipid multilayers, except at the membrane surface where residual protein appears to be concentrated. The additional density at the boundaries between the compacted membrane bi-layers could be due, in part, to the basic proteins associated with negatively charged lipid polar groups. Since it is unlikely that there is much protein penetrating the hydrocarbon layer, the unequal steps that border the low density trough in the compacted membrane profile (Fig. 10) may represent an unequal distribution of cholesterol as previously suggested for the native membrane (5).

### *Molecular Changes on Freezing Compact Myelin*

Compact myelin membranes show a negative thermal expansion (Fig. 10 and reference 12) similar to that for model lipid systems (15, 19). Since we have measured the diffraction only at room temperature and liquid nitrogen temperature, we cannot calculate a meaningful thermal expansion coefficient. It appears, however, that as the temperature is lowered, the hydrocarbon chains stiffen, but once they reach a fully extended conformation, the negative thermal expansion will diminish. On the external side of the membrane bilayer, the structural change with freezing is just an expansion. On the cytoplasmic side, however, there is, in addition, a small change in the shape of the bilayer in which electron-dense material is being displaced from the step region to the peak region. As the hydrocarbon chains stiffen on lowering the temperature, the high density portions of cholesterol and lipid polar groups may be shifted away from the step region into the polar group layer. The greater thermal lability on the side of the lipid bilayer with lower cholesterol content is consistent with observations on model lecithin-bilayers containing different proportions of cholesterol (19).

We have used x-ray diffraction and freeze-fracture electron microscopy to provide complementary information on structural heterogeneity in myelin and on the extent of structural preservation by freezing. The x-ray patterns show that the peroidicity and regularity in the membrane arrays are retained when frozen from saline solution with 20% DMSO or glycerol, but without cryoprotection the structure is disordered. Freeze-fracture replicas of myelin treated with DMSO establish that the compacted membrane arrays are formed by localized recrystallization and are continuous with native period domains in the myelin sheath. Myelin in glycerol has been found to undergo a transient compaction that can be trapped by freezing. Electron density profiles of compacted myelin membranes that have been frozen show that there is a small, negative thermal expansion of the membrane unit and some reorganization in the cytoplasmic half of the membrane bilayer. The asymmetry in the hydrocarbon layer of compacted myelin membranes, which appear particle-free in freeze-fracture replicas, can be accounted for by a nonuniform distribution of cholesterol in the bilayer. Our study demonstrates that a correspondence can be established between the membrane arrays seen by electron microscopy of freeze-fractured specimens and the periodic structures revealed by x-ray diffration.

We would like to thank Dr. Walter Phillips for setting up the point-focus x-ray cameras, William Saunders for assistance with the photography, and Dr. Allen Ganser for his helpful comments on the manuscript.

This work was supported by National Institutes of Health grants NS13408 and NS14326 (D. A. Kirschner), and CA15468 (D. L. D. Caspar), and National Science Foundation grant PCM77-13955 (D. L. D. Caspar and D. A. Goodenough).

*Received for publication 11 December 1978.*

## REFERENCES


1. BENITEZ, C., D. L. D. CASPAR, and D. A. KIRSCHNER. 1977. Freeze-fracture studies of particle segregation in compacted myelin. Proceedings of the 35th Annual Meeting, Electron Microscopy Society of America. Claitors, Baton Rouge, La. 600–601.
2. BRANTON, D. 1967. Fracture faces of frozen myelin. *Exp. Cell. Res.* **45:** 703–707.
3. BRAUN, P. E., and S. W. BROSTOFF. 1977. Proteins of myelin. *In* Myelin. P. Morell, editor. Plenum Press, New York. 201–231.
4. BROSTOFF, S. W., Y. D. KARKHANIS, D. J. CARLO, W. REUTER, and E. H. EYLAR. 1975. Isolation and partial characterization of the major proteins of rabbit sciatic nerve myelin. *Brain Res.* **86:**449–458.
5. CASPAR, D. L. D., and D. A. KIRSCHNER. 1971. Myelin membrane structure at 10 Å resolution. *Nat. New Biol.* **231:**46–52.
6. COSTELLO, M. J., and T. GULIK-KRZYWICKI. 1976. Correlated X-ray diffraction and freeze-fracture studies on membrane model systems: Perturbations induced by freeze-fracture preparative procedures. *Biochim. Biophys. Acta.* **455:**412–432.
7. EVERLY, J. L., R. O. BRADY, and R. H. QUARLES. 1973. Evidence that the major protein in rat sciatic nerve myelin is a glycoprotein. *J. Neurochem.* **21:**329–334.
8. FRANKS, N. P. 1976. Structural analysis of hydrated egg lecithin and cholesterol bilayers. I. X-ray diffraction. *J. Mol. Biol.* **100:**345–358.
9. GREENFIELD, S., S. BROSTOFF, E. H. EYLAR, and P. MORELL. 1973. Protein composition of myelin of the peripheral nervous system. *J. Neurochem.* **20:**1207–1216.
10. HEUSER, J. E. 1977. Quick-freezing to catch the membrane changes that occur during exocytosis. Proceedings of the 35th Annual Meeting, Electron Microscopy Society of America. Claitors, Baton Rouge, La. 676–679.
11. KIRSCHNER, D. A. 1974. Comparative X-ray and neutron diffraction from nerve myelin membranes. *In* Spectroscopy in Biology and Chemistry. S. Yip and S.-H. Chen, editors. Academic Press, Inc., New York. 203–233.
12. KIRSCHNER, D. A., and D. L. D. CASPAR. 1975. Myelin structure transformed by dimethylsulfoxide. *Proc. Natl. Acad. Sci. U. S. A.* **72:** 3513–3517.
13. KIRSCHNER, D. A., D. L. D. CASPAR, B. P. SCHOENBORN, and A. C. NUNES. 1975. Neutron diffraction studies of nerve myelin. *In* Neutron Scattering for the Analysis of Biological Structures. B. P. Schoenborn, editor. Brookhaven Symposium in Biology, No. 27, III. 68–76.
14. KITAMURA, K., K. SUZUKI, and K. UYEMURA. 1976. Purification and partial characterization of two glycoproteins in bovine peripheral nerve myelin membrane. *Biochim. Biophys. Acta.* **455:**806–816.
15. LUZZATI, V., H. MUSTACCHI, A. SKOULIOS, and F. HUSSON. 1960. La structure des colloïdes d'association. I. Les phases liquid-cristallines des systèmes amphiphile-eau. *Acta. Crystallogr. Sect. B.* **13:**660–667.
16. MCINTOSH, T. J. 1978. The effect of cholesterol on the structure of phosphatidylcholine bilayers. *Biochim. Biophys. Acta.* **513:**43–58.
17. PINTO DA SILVA, P., and R. G. MILLER. 1975. Membrane particles on fracture faces of frozen myelin. *Proc. Natl. Acad. Sci. U. S. A.* **72:**4046–4050.
18. RAND, R. P., and V. LUZZATI. 1968. X-ray diffraction study in water of lipids extracted from human erythrocytes: The position of cholesterol in the lipid lamellae. *Biophys. J.* **8:**125–137.
19. RAND, R. P., and W. A. PANGBORN. 1973. A structural transition in egg lecithin-cholesterol bilayers at 12°C. *Biochim. Biophys. Acta.* **318:**299–305.
20. WILKINS, M. H. F., A. E. BLAUROCK, AND D. M. ENGELMAN. 1971. Bilayer structure in membranes. *Nat. New Biol.* **230:**72–76.
21. WOOD, J. G., and R. M. C. DAWSON. 1973. A major myelin glycoprotein of sciatic nerve. *J. Neurochem.* **21:**717–719.
22. ZINGSHEIM, H. P., and H. PLATTNER. 1976. Electron microscopic methods in membrane biology. *In* Methods in Membrane Biology. Vol. 7. E. Korn, editor, Plenum Press, New York. 1–146.